Cell migration driven by substrate deformation gradients

Susana Márquez[1], German Reig[2,3], Miguel Concha[4], and Rodrigo Soto[1]

[1] Departamento de Física, FCFM, Universidad de Chile, Santiago, Chile.
[2] Universidad Bernardo OHiggins, Escuela de Tecnología Médica and Centro Integrativo de Biología y Química Aplicada (CIBQA), Santiago, Chile.
[3] Instituto de Ciencias Biomédicas (ICBM), Facultad de Medicina, Universidad de Chile, Santiago, Chile.
[4] BNI, Facultad de Medicina, Universidad de Chile, Santiago, Chile.

E-mail: `rsoto@dfi.uchile.cl`

Abstract. Identifying the cues followed by cells is key to understand processes as embryonic development, tissue homeostasis, or several pathological conditions. Based on a durotaxis model, it is shown that cells moving on predeformed thin elastic membrane follow the direction of increasing strain of the substrate. This mechanism, straintaxis, does not distinguish the origin of the strain, but the active stresses produce large strains on cells or tissues being used as substrates. Hence, straintaxis is the natural realization of duratoaxis in vivo. Considering a circular geometry for the substrate cells, it is shown that if the annular component of the active stress component increases with the radial distance, cells migrate toward the substrate cell borders. With appropriate estimation for the different parameters, the migration speeds are similar to those obtained in recent experiments [Reig *et al.* Nat. Comm. 2017, **8**, 15431]. In these, during the annual killifish epiboly, deep cells that move in contact with the epithelial enveloping cell layer (EVL), migrate toward the EVL cell borders with speeds of microns per minute.

Keywords: cell migration, durotaxis, mechanosensing

Submitted to: *Phys. Biol.*

1. Introduction

The movement of cells, either as individuals or as collectives, is critical not only for embryonic development and tissue homeostasis but also in the origin and progression of several pathological conditions such as cancer [for review, see [1, 2, 3]]. Cells are able to migrate in microenvironments with different physical and chemical properties showing adaptive behaviors. On two-dimensional (2D) culture dishes, cells frequently show extensive lamellipodia and strong adhesion with the substrate while they produce blebs and exhibit only mild substrate adhesion when immersed in three-dimensional (3D) matrix gels [4, 5, 6]. Importantly, transition between these two types of migration can be triggered by changing the mechano-chemical properties of the substrate and/or by modulating the adhesive/contractile state of the cell [7]. For instance, changing cell contractility by modulating the actomyosin cytoskeleton leads to transitions between blebs and lamellipodial-mediated migration in tumor cell lines in culture [8]. Classically, individual cell migration has been studied in 2D culture dishes coated with different extracellular matrix (ECM) components, describing a cycle of events that leads to cell crawling [9]. In the cycle, cells first polarize and produce cellular protrusions that stabilize at the front upon interaction with ECM molecules such as Fibronectin, forming macromolecular protein complexes called focal adhesions [10]. Using these cell-ECM contacts as anchors the cell moves along the axis of polarity by detachment of the rear side to then start a new cycle of adhesion at the front [10]. In contrast to 2D culture dishes, cell movement within living tissues is not restricted to ECM contacts but cells can also use other cells as substrate for migration [6, 11]. Several external guiding cues provide directionality to the cell movement. Often, cells move along gradients of diffusible chemical signals (chemotaxis) but they can also follow gradients of electric potential (galvanotaxis) and substrate stiffness (durotaxis) [12, 13, 14]. Direct evidence of durotaxis has been obtained using in vitro experiments, where a mesenchymal cell is placed on a substrate with an inhomogeneous Young modulus, either in the form of a step function [13] or with a smooth gradient [15]. In both cases, it has been observed that mesenchymal cells migrate preferentially toward the regions of higher stiffness. Several models have been proposed to explain and describe durotaxis [16, 17, 18]. In Ref. [19], it is found that for focal adhesions, the force exerted on a protrusion and the retraction velocity are proportional, with a constant that increases with the local effective stiffness of the substrate which, in turn, is proportional to the substrate Young modulus. Hence, if protrusions on opposite sides of the cell are in contact with substrates of different Young moduli, they are able to locally sense the stiffness difference and generate a net migration velocity.

Recently, in vivo experiments performed in early embryos of annual killifish showed that mesenchymal-like cells of the embryonic deep cell layer (DCL) migrate using the upper epithelial enveloping cell layer (EVL) as substrate [20]. The authors reported that, although DCL cells are able to move autonomously in a random fashion, they become preferentially located towards EVL cell borders [20]. Discarding other signals,

such as chemical, as driving force and supported by results showing that mechanical manipulations can disrupt DCL topology, the authors strongly suggested a mechanical signal as a driving force. Specifically, increased tension/stiffness at EVL cell borders, compared to the center of the cell, was proposed to be sensed by DCL cells to direct their migration [20]. However, the migration process of DCL cells starts much before they touch the EVL cell borders and thus sense the differences in stiffness, being therefore unable to describe this migration by the usual durotaxis model. For thin elastic membranes such as the EVL cell layer, the effective stiffness is proportional to the membrane thickness times the Young modulus [21]. Hence, following the argumental line of Ref. [19] it would also result in a migrating process in the direction of higher thickness. The experiments reported in Ref.[20] show precisely the opposite as the EVL cell borders are thinner. However, there is an important difference between the in vivo and in vitro experiments of durotaxis as in the former, the substrate is not a passive elastic medium but rather, active stresses are present [22]. These active stresses, generated by the cortical actin ring and cytoskeleton of EVL cells, deform the substrate. In this article we show that when these deformations are large as it is indeed the case for the reported experiment, the effective stiffness of a thin membrane depends also on the equilibrium deformation. As DCL cells sense the effective stiffness, nonuniform deformations of the substrate can generate a mechanically induced migration toward regions of larger strain, even if the substrate has a uniform Young modulus.

The article is organized as follows. In section 2 we extend the durotaxis model of Refs. [23, 19] to the case of thin membranes. Section 3 presents the derivation of the effective stiffness for substrates subject to active stresses. A simple cell model is presented in section 4 showing that reasonable values for the deformation field produce migration speeds that are of the same order as the observed ones. Finally, a discussion on the model and possible ways it could be verified experimentally are presented in section 5.

2. Durotaxis over thin elastic substrates

The process of single cell migration we aim to describe takes place in a confined space between the epithelial EVL and the yolk cell of the early annual killifish embryo. Here, mesenchymal DCL cells use the inner (basal) surface of the EVL to migrate, where the protrusions adhere, while the yolk cell plays primarily a passive frictional role [20] (see figure 1 for a sketch). The outer (apical) surface of the EVL is stress-free. The typical thicknesses of the EVL is just a few micrometers, while the lateral size of the migrating DCL cells is much larger, of the order of tens of micrometers. Also the lateral extension of the protrusions are larger than the EVL thickness. Therefore, for the purpose of computing the elastic response of the EVL, at distances larger than the thickness, it can be modeled as a thin elastic plate. Hence, we first extend the durotaxis models presented in Refs. [23, 19], originally developed for semi-infinite substrates, to this geometry. We consider a flat membrane of thickness h, oriented along the x and y directions, subject

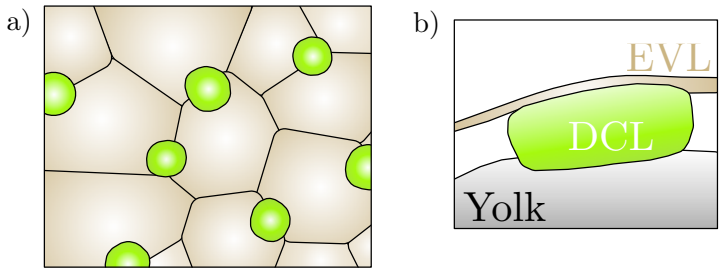

Figure 1. Sketch of the system under consideration. In green, the mesenchymal deep cells (DCL), in brown, the epithelial enveloping cell layer (EVL), and in gray, the yolk cell. a) Frontal view. b)Lateral view.

to surface forces densities $\mathbf{f}$ in the planar directions. The displacement vector field $\mathbf{u}$ is obtained from the elastic equations for thin plates of finite but small thickness [21]

$$(1-\nu)\frac{\partial^2 u_i}{\partial r_k^2} + (1+\nu)\frac{\partial^2 u_k}{\partial r_k \partial r_i} = \frac{-2\,(1-\nu^2)}{Eh} f_i(\mathbf{r}), \tag{1}$$

where E is the substrate Young modulus, ν is the Poisson ratio, and i and k are the Cartesian coordinates in the plane. Here and in the subsequent expressions, Einstein notation is used. For a concentrated force exerted by a cell protrusion $\mathbf{f}(\mathbf{r}) = \mathbf{F}\delta^{(2)}(\mathbf{r})$, the solution of (1) is

$$u_i(\mathbf{r}) = \frac{(1+\nu)}{4\pi Eh}\left[(\nu-3)\ln\left(\frac{|\mathbf{r}|}{a}\right)\delta_{ik} + \frac{(1+\nu)}{|\mathbf{r}|^2} r_i r_k\right] F_k, \tag{2}$$

where a is a length scale, which as usual in two dimensions, must be fitted using external boundary conditions at a finite distance. In the case of an epithelium, this boundary condition is naturally placed at the cell borders. The use of Dirac delta distribution for the force, produces a displacement field that diverges at the origin. To obtain the displacement generated by a protrusion of radius R_1 (see figure 2a for a sketch), equation (2) is averaged over the area of the protrusion, resulting in the finite displacement

$$\langle \mathbf{u} \rangle = \frac{3\ln(R_1/a)}{8\pi Eh}\mathbf{F} = \kappa_c^{-1}\mathbf{F}, \tag{3}$$

which defines the effective stiffness κ_c of the substrate. We remark that it is proportional to the membrane thickness and Young's modulus. This is opposite to what happens when the substrate in strongly anchored in the bottom, in which case the effective stiffness grows when decreasing h [24, 25].

With the effective stiffness it is possible to find a relation between the retraction speed $\mathbf{V}$ of a protrusion and the average force $\mathbf{F}$ it exerts on the substrate due to adhesion molecules [19]. Under the condition that these molecules are in a dynamic state, where attachment and detachment processes are equilibrated, it was found that for small velocities, $\mathbf{F} = b\mathbf{V}$, with

$$b = N_{\mathrm{ac}}\frac{k_a}{k_d^0}\left(\frac{1}{k_a + k_d^0}\right)\frac{\kappa_c}{1+\kappa_c/\bar{\kappa}} \equiv b_0\frac{\kappa_c}{1+\kappa_c/\bar{\kappa}}. \tag{4}$$

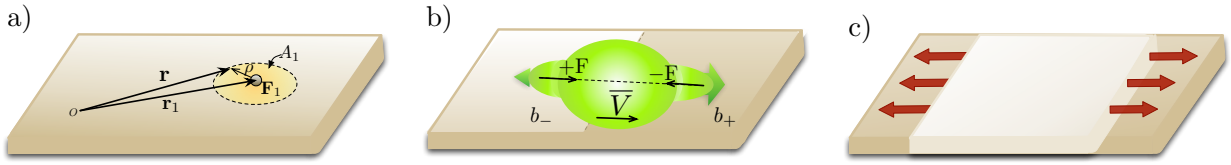

Figure 2. a) A thin membrane under a concentrated force $\mathbf{F}_0$ in the planar directions. The circle of radius R_1 represents the protrusion zone where the displacement field is averaged. b) A cell with attachment points on its opposite sides, exert opposite and equal forces on the substrate. c) Substrate subject to an homogeneous uniaxial deformation.

Here, $N_{\rm ac}$ is the number of adhesion molecules per adhesion complex, k_a and k_d^0 are the molecular binding and unbinding rates, and $\bar{\kappa}$ is the composite stiffness of the extra cellular matrix and the adhesion molecules. Importantly, b is a monotonic increasing function of κ_c and, therefore, the force needed to retract the protrusion increases with both E and h.

With these elements, it is now possible to understand the first phase of durotaxis, before the migrating cells become polarized. For simplicity, we consider just two protrusions acting on opposite sides of the cell. These protrusions are mechanically linked by the cytoskeleton within the cell and, by mechanical equilibrium, exert the same but opposite force $\mathbf{F}$ (see figure 2b). If protrusions locate over regions where the substrate has different Young moduli or thicknesses (hence, different values of b), the retraction velocities will be different and the cell center will move with a speed

$$\overline{V} = \frac{V_+ - V_-}{2} = \frac{F}{2}\left(\frac{1}{b_+} - \frac{1}{b_-}\right) \tag{5}$$

in the direction of higher values of Eh. This is the linear process of durotaxis. Later, once the cell starts to make adhesions to the substrate, the cytoskeleton will align in this direction, provoking the cell polarization.

3. Response of an already deformed substrate

The epithelial cell that acts as substrate is subject to active stresses generated by its own cytoskeleton and those of neighboring epithelial cells. Already in absence of external forces exerted by the DCL, these active stresses generate a base deformation of the substrate, described by a displacement vector field $\mathbf{u}^{(0)}$. The active stresses in a substrate cell $\sigma_{ik}^{\rm A}$ balance with the elastic ones $\sigma_{ik}^{\rm E}$, such that the total stress tensor $\sigma_{ik}^{\rm T} = \sigma_{ik}^{\rm A} + \sigma_{ik}^{\rm E}$ obeys the equation for mechanical equilibrium

$$\frac{\partial \sigma_{ik}^{\rm T}}{\partial r_k} = 0, \tag{6}$$

with some boundary conditions imposed by the neighbor cells. The molecular motors generate active stresses that are contractile and, as evidenced by laser ablation experiments [26], they are strong enough to deform the epithelial cells by an important

fraction. Under these conditions, it is not sufficient to consider the linear approximation for the strain tensor, and the full expression in terms of the displacement vector must be used

$$u_{ik}^{(0)} = \frac{1}{2}\left(\frac{\partial u_i^{(0)}}{\partial r_k} + \frac{\partial u_k^{(0)}}{\partial r_i} + \frac{\partial u_l^{(0)}}{\partial r_k}\frac{\partial u_l^{(0)}}{\partial r_k}\right). \tag{7}$$

In this article, we will assume that the elastic stresses are Hookean despite the large deformations. Nonlinear relations could be necessary to describe fully the epithelium but they will only change quantitatively the main conclusions of this manuscript, namely that the large deformations can lead to directed cell migration. Hence, we consider the linear expression for elastic stress for thin plates under longitudinal deformations [21]

$$\sigma_{ik}^{\mathrm{E}} = \frac{E\nu}{1-\nu^2}\delta_{ik}u_{ll}^{(0)} + \frac{E}{1+\nu}u_{ik}^{(0)}. \tag{8}$$

In principle, the non-linear set of equations (6), (7), and (8) allow the computation of $\mathbf{u}^{(0)}$ for a given distribution of active stresses.

The reference state proved by the migrating cells is $\mathbf{u}^{(0)}$. Under the action of the protrusion forces $\mathbf{f}$ in addition to the active stresses, the epithelium will now experience a total displacement $\mathbf{u} = \mathbf{u}^{(0)} + \mathbf{u}^{(1)}$, where $\mathbf{u}^{(1)}$ is the additional displacement produced by the protrusions. When mesenchymal cells migrate over the epithelium, no deformation of the later is visible in experiments, from where we can deduce that the protrusion forces are much weaker than those that result from the internal active stresses [27]. Hence, we can consider that $|\mathbf{u}^{(1)}| \ll |\mathbf{u}^{(0)}|$, as well as for their gradients. Then, the equilibrium equation for $\mathbf{u}^{(1)}$ can be linearized, resulting in

$$\begin{aligned}(1-\nu)\frac{\partial^2 u_i^{(1)}}{\partial r_k^2} + (1+\nu)\frac{\partial^2 u_k^{(1)}}{\partial r_k \partial r_i} + 2\nu\Big(\frac{\partial u_j^{(0)}}{\partial r_l}\frac{\partial^2 u_j^{(1)}}{\partial r_i \partial r_l} + \frac{\partial u_j^{(1)}}{\partial r_l}\frac{\partial^2 u_j^{(0)}}{\partial r_i \partial r_l}\Big)\\ +(1-\nu)\Big(\frac{\partial u_j^{(0)}}{\partial r_k}\frac{\partial^2 u_j^{(1)}}{\partial r_k \partial r_i} + \frac{\partial u_j^{(1)}}{\partial r_k}\frac{\partial^2 u_j^{(0)}}{\partial r_k \partial r_i}\\ +\frac{\partial u_j^{(0)}}{\partial r_i}\frac{\partial^2 u_j^{(1)}}{\partial r_k^2} + \frac{\partial u_j^{(1)}}{\partial r_i}\frac{\partial^2 u_j^{(0)}}{\partial r_k^2}\Big) = \frac{-2\,(1-\nu^2)}{Eh}f_i(\mathbf{r}).\end{aligned} \tag{9}$$

As $\mathbf{u}^{(0)}$ is a function of σ_{ik}^{A}, the elastic response given by (9) depends effectively on the active stresses of the epithelium.

Despite its apparent complexity, (9) can be solved for the illustrative case of an homogeneous uniaxial deformation $\mathbf{u}^{(0)}(\mathbf{r}) = \epsilon x\hat{x}$, where ϵ (not necessarily small) is the strain, shown in figure 2c. Solving iteratively in powers of ϵ and then resumming the resulting series, it is found for a concentrated force $\mathbf{f}(\mathbf{r}) = \mathbf{F}\delta(\mathbf{r})$ that the total displacement is

$$u_i^{(1)}(\mathbf{r}) = \frac{(1+\nu)}{4\pi Eh}\Big[(\nu-3)\ln\left(\frac{|\mathbf{r}|}{a}\right)\delta_{ik} + \frac{(1+\nu)}{|\mathbf{r}|^2}r_i r_k\Big]\Big(1 - \frac{\epsilon\delta_{xk}}{1+\epsilon}\Big)F_k. \tag{10}$$

We note that the response is anisotropic. Performing the same averaging procedure as in section 2, the effective stiffness in the two principal directions are

$$\kappa_{c,x} = \frac{8\pi Eh(1+\epsilon)}{3\ln(R_1/a)}, \kappa_{c,y} = \frac{8\pi Eh}{3\ln(R_1/a)}, \tag{11}$$

which depend on the preexisting deformation of the substrate. In particular, κ_c depends on the sign of ϵ, that is, if the membrane has been previously stretched or compressed. It is found that the substrate is harder to deform in the direction of the active strain when $\epsilon > 0$, that is, when it is under the action of contractile active stresses. The origin of this result is not immediate because it originates in the geometric non-linearity present in (7).

As migrating cells sense the local stiffnesses κ_c, plugging (11) into (4) and (5), implies that a cell generating protrusions on a predeformed substrate, will move toward the regions of larger strains ϵ, presenting, what we call, *straintaxis*. Note that what the migrating cell effectively responds to is the deformation strain of the substrate and not the active stresses or the boundary conditions that generate them.

4. Model for an epithelial substrate

Recent experiments suggest that mesenchymal DCL cells migrate over the inner surface of the EVL toward the borders of epithelial cells (see figure 3 and Ref. [20]). Here, we aim to analyze if it is plausible that this migration can be described as a straintaxis.

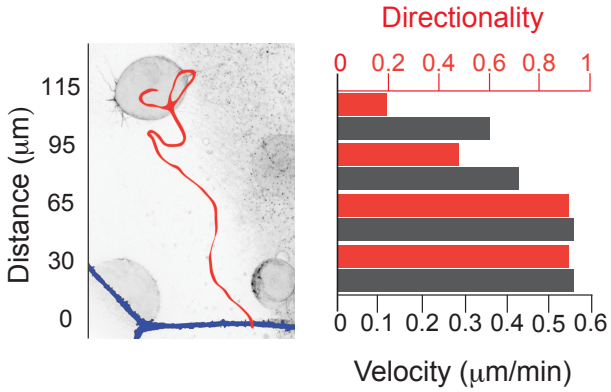

Figure 3. Left: Confocal microscopy z-stack maximum projection of an embryo. The red line corresponds to the track followed by the cell as it approaches the border during a period of 45 min. Numbers on the left indicate the distance to the substrate cell border (distance=0), used to define intervals for the quantifications shown in the right figure. Right: Quantification of the velocity (dark brown) and directionality (red) of the cell movement. Reproduced from Ref. [20] (CC BY 4.0).

We first analyze if it is possible that contractile active stresses generate deformations where the strain increases when approaching the cell borders. For simplicity, we approximate the polygonal shape of the epithelium cells to a circle of radius R, where the symmetry allows to make simple models (see figure 4a). For a radially deformed epithelial cell $\mathbf{u}^{(0)} = u(r)\hat{\mathbf{r}}$, the deformation gradient in polar coordinates is $\nabla\mathbf{u}^{(0)} = \frac{du}{dr}\hat{\mathbf{r}}\hat{\mathbf{r}} + \frac{u}{r}\hat{\boldsymbol{\phi}}\hat{\boldsymbol{\phi}}$, resulting in the following nonvanishing components of the strain tensor (7), $u_{rr} = \frac{du}{dr} + \frac{1}{2}\left(\frac{du}{dr}\right)^2$ and $u_{\phi\phi} = u/r + \frac{1}{2}(u/r)^2$. With the help of (8), the nonvanishing components of the elastic stress tensor are $\sigma^{\mathrm{E}}_{rr} = \frac{E}{1-\nu^2}(u_{rr} + \nu u_{\phi\phi})$ and $\sigma^{\mathrm{E}}_{\phi\phi} = \frac{E}{1-\nu^2}(u_{\phi\phi} + \nu u_{rr})$.

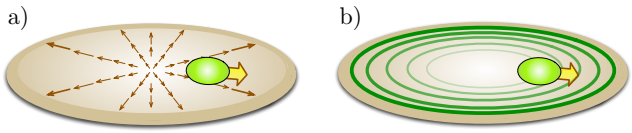

Figure 4. a) Substrate cell modeled as a circle, subject to an inhomogeneous deformation profile. b) Contractile annular alignment of the active stresses that give rise to radially increasing strains. In both panels the light green circle represents mesenchymal cell moving in contact with the substrate and the yellow arrow, the resulting migrating direction.

Because the substrate is in mechanical equilibrium, (6) must be fulfilled, resulting in the following equation for the active stresses,

$$\frac{1}{r}\frac{d}{dr}(r\sigma^{\mathrm{A}}_{rr}) - \frac{\sigma^{\mathrm{A}}_{\phi\phi}}{r} = \frac{E}{1+\nu}\frac{(u_{\phi\phi}-u_{rr})}{r} - \frac{E}{1-\nu^2}\frac{d}{dr}(u_{\phi\phi}+u_{rr}), \tag{12}$$

where we used that for tensors with radial symmetry, $\nabla\cdot\boldsymbol{\sigma} = \left[\frac{1}{r}\frac{d}{dr}(r\sigma_{rr}) - \frac{1}{r}\sigma_{\phi\phi}\right]\hat{\mathbf{r}}$.

We first note that if the substrate is deformed only by the action of neighbor epithelial cells and the actine ring on its border, no straintaxis can take place. Indeed, in this case, $\sigma^{\mathrm{A}}_{rr} = \sigma^{\mathrm{A}}_{\phi\phi} = 0$ in the bulk and the solution of (12) is a linear deformation profile $u = \lambda r$. Then, the strain tensor is uniform and no migration can take place. Hence, to generate straintaxis, active stresses inside the cell must take place or, equivalently, u must be nonlinear. Instead of solving (12) for giving forms of σ^{A}, we model u in the simplest nonlinear form $u = u_{\max}(r/R)^2$, where $u_{\max}$ gives the deformation at the cell border, and deduce from (12) the structure of σ^{A}. As we have one equation but two unknowns, we must model the anisotropy of the active stress tensor. This is linked to the microstructure of the cytoskeleton network, which is known to be highly anisotropic. Three limiting cases are considered: either there is complete isotropy $\sigma^{\mathrm{A}}_{rr} = \sigma^{\mathrm{A}}_{\phi\phi}$ or one component of the tensor vanishes representing a cytoskeleton with fibers perfectly aligned, $\sigma^{\mathrm{A}}_{rr} = 0$ or $\sigma^{\mathrm{A}}_{\phi\phi} = 0$. For the isotropic case the solution is

$$\sigma^{\mathrm{A}}_{rr} = \sigma^{\mathrm{A}}_{\phi\phi} = -\frac{Eu_{\max}r}{(1-\nu^2)R^2}\left[3 + (11-\nu)\frac{u_{\max}r}{4R^2}\right], \tag{13}$$

where we imposed that $\sigma^{\mathrm{A}}_{rr}(r=0) = 0$. For $\sigma^{\mathrm{A}}_{\phi\phi} = 0$,

$$\sigma^{\mathrm{A}}_{rr} = -\frac{Eu_{\max}r}{(1-\nu^2)R^2}\left[\frac{3}{2} + (11-\nu)\frac{u_{\max}r}{6R^2}\right]. \tag{14}$$

In these two cases, the stresses result to be extensile (i.e. σ_{rr} and $\sigma_{\phi\phi}$ are negative) and therefore, should be discarded. Finally, for the annular alignment of the cytoskeleton (see figure 4b), $\sigma^{\mathrm{A}}_{rr} = 0$,

$$\sigma^{\mathrm{A}}_{\phi\phi} = \frac{Eu_{\max}r}{(1-\nu^2)R^2}\left[3 + (11-\nu)\frac{u_{\max}r}{2R^2}\right], \tag{15}$$

which is indeed contractile (i.e. $\sigma_{\phi\phi}$ is positive). Hence, an annular organization of the cytoskeleton, with more activity near the borders, generate strains with gradients pointing in the outward direction as shown in figure 4, being good candidates to account

for the cell migration. This organization of contractile active stresses at the borders has also been observed in small cell colonies [28].

In order for this mechanism to be a possible responsible of the observed migration, the migration speeds must be of the order of the reported values: fraction of a μm/min (figure 3). Equations (4), (5), and (11) give for the migration speed

$$\bar{V} = \frac{3F}{16\pi}\frac{\log(R_1/a)}{b_0 hE}\Big(\frac{1}{1+\epsilon_+} - \frac{1}{1+\epsilon_-}\Big). \tag{16}$$

Here, the driving force for the radial motion is $\epsilon = u_{rr} = 2u_{\max}r/R^2 + 2u_{\max}^2 r^2/R^4$, which must be evaluated on the extremes of the migrating cell. To estimate the resulting speed, several considerations are made. First, for the different constants appearing in evaluating b_0 in (4), we take the same values as in Ref. [19]: number of adhesion molecules per adhesion complex, $N_{\rm ac} \approx 10^3$; unstrained binding rates of adhesion complex-extra cellular matrix (AC-ECM), $k_0^a \approx 1\mathrm{s}^{-1}$; unstrained off rates of AC-ECM, $k_0^d \approx 1\mathrm{s}^{-1}$; composite stiffness of adhesion-ECM molecule, $\bar{\kappa} \approx 25\mathrm{pNnm}^{-1}$; exerted force, $F \approx 500\mathrm{pN}$. Note that many of these values were mere orders of magnitude estimations. Second, we consider the reported migration in Ref. [20], to estimate the substrate Young's modulus, $E \approx 20\mathrm{kPa}$; substrate thickness, $h \approx 1\,\mu$m; migrating cell radius, $R_{\rm migrating} \approx 30\,\mu$m; radius of adhesion patch, $R_1 \approx 5\,\mu$m; and the radius of the enveloping layer cells that serve as substrate, $R = 300\,\mu$m. Finally, we took $a = 1\,\mu$m.

Figure 5 presents the migration speed as a function of the distance to the substrate cell center, for various values of $u_{\max}$, which quantifies the deformation of the substrate. The resulting speeds are one order of magnitude smaller than the experimental values (see figure 3 for comparison). This can be due to the crude estimations used for the parameters of the model, but we prefer to keep the values of Refs. [19, 20] in absence of precise experimental values. Additionally, the migration to the borders was observed for many cells, but the quantification of the speed was made for only one cell, lacking therefore more precise data to compare with. Note finally that the predicted speed decreases with distance. This a result of the saturation of b with increasing values of κ_c.

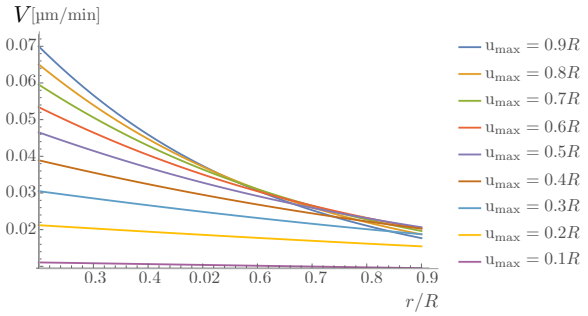

Figure 5. Migration speed as a function of cell mass center position. The different colors show the behavior for different values of $u_{\max}$.

5. Conclusions and discussion

In durotaxis, cells migrate in the direction of increasing effective stiffness of the substrate. In this article we have shown that the effective stiffness of predeformed thin elastic membranes increases with the strain and, therefore, cells migrate toward regions on higher strains of the substrate. The mechanism does not distinguish the origin of this deformation but, at least for uniaxial or circular geometries, boundary effects give rise only to uniform strains. Hence, the active stresses generated by the cytoskeleton in epithelial substrates are the most natural origin of nonuniform strains which, also, are known to be large. The migration by strain gradients, straintaxis, is consequently a relevant realization of durotaxis is vivo. To quantify its importance compared to the effect of gradients in Young modulus, a difficulty of in vivo experiments must be overcome, which is the inability to directly measure the Young modulus. Instead, what is measured is the effective stiffness that correlates local deformations with the applied force [29], which we showed depends on the Young modulus, thickness and the strain. The deformation field in tissues, on the other hand, can be measured using traction force microscopy, tracking the temporal evolution of the tissue, or by laser ablation. Finally, straintaxis can be tested in vitro with synthetic predeformed substrates, with the precaution of maintaining the thin film approximation and using nonuniform deformations. Strained substrates can also reorient cells [30, 31]. Further studies are needed to elucidate the possible interplays between this reorientation and the migration of cells by the mechanism described here.

Modeling the epithelial cells used as a substrate for migration with a circular geometry, we showed that annular oriented contractile stresses, increasing toward the border, can induce the directional motion of mesenchymal cells. The resulting speeds, using crude estimations of the parameters, are one order of magnitude smaller than recently reported results. This opens the need to measure in detail the different mechanical terms involved in the model, by directly probing focal cell-substrate complexes. The model also predicts that the elastic properties of the substrate cells are anisotropic, feature that could be directly verified in experiments using, for example, atomic force microscopy.

In the manuscript, we have assumed a Hookean elastic response of the substrate. It is known that the cytoskeleton can present nonlinear elasticity. In a simple scalar form, $\sigma \sim Eu + E^{(2)}u^2$, with $E^{(2)} > 0$, indicating that the substrate becomes stiffer under strain. By the arguments presented here, with the model of active stresses discussed in section 4, the migration would also be toward the cell borders. Further experiments are needed to quantify the relative importance of the nonlinear elasticity compared to straintaxis.

Acknowledgments

This work was supported by the Chilean Millennium Science Initiative (Millennium Nucleus on "Physics of active matter" to R.S., S.M., and M.L.C., and Millennium Institute P09-015-F to M.L.C.) and the Chilean National Commission for Scientific and Technological Research (Ring Initiative ACT1402 to M.L.C., R.S., and G.R., FONDAP 15150012 to M.L.C.; FONDECYT 11170761 and PAI 79170126 to G.R.; FONDECYT 1180791 to R.S. and S.M.; and Conicyt PFCHA Magister Nacional Scholarship 2016 for SM).

[1] Franz C M, Jones G E and Ridley A J 2002 *Developmental cell* **2** 153–158
[2] Qu F, Guilak F and Mauck R L 2019 *Nature Reviews Rheumatology* 1
[3] Yamaguchi H, Wyckoff J and Condeelis J 2005 *Current opinion in cell biology* **17** 559–564
[4] Cukierman E, Pankov R, Stevens D R and Yamada K M 2001 *Science* **294** 1708–1712
[5] Webb D J and Horwitz A F 2003 *Nature Cell Biology* **5** 690
[6] Reig G, Pulgar E and Concha M L 2014 *Development* **141** 1999–2013
[7] Petrie R J, Gavara N, Chadwick R S and Yamada K M 2012 *J Cell Biol* **197** 439–455
[8] Bergert M, Chandradoss S D, Desai R A and Paluch E 2012 *Proceedings of the National Academy of Sciences* **109** 14434–14439
[9] Ridley A J, Schwartz M A, Burridge K, Firtel R A, Ginsberg M H, Borisy G, Parsons J T and Horwitz A R 2003 *Science* **302** 1704–1709
[10] Parsons J T, Horwitz A R and Schwartz M A 2010 *Nature reviews Molecular cell biology* **11** 633
[11] Richardson B E and Lehmann R 2010 *Nature reviews Molecular cell biology* **11** 37
[12] Brown M J and Loew L M 1994 *The Journal of cell biology* **127** 117–128
[13] Lo C M, Wang H B, Dembo M and Wang Y l 2000 *Biophysical journal* **79** 144–152
[14] Cortese B, Palama I E, D'Amone S and Gigli G 2014 *Integrative Biology* **6** 817–830
[15] Isenberg B C, DiMilla P A, Walker M, Kim S and Wong J Y 2009 *Biophysical journal* **97** 1313–1322
[16] Stefanoni F, Ventre M, Mollica F and Netti P A 2011 *Journal of theoretical biology* **280** 150–158
[17] Allena R, Scianna M and Preziosi L 2016 *Mathematical biosciences* **275** 57–70
[18] Aubry D, Gupta M, Ladoux B and Allena R 2015 *Physical biology* **12** 026008
[19] Harland B, Walcott S and Sun S X 2011 *Physical biology* **8** 015011
[20] Reig G, Cerda M, Sepúlveda N, Flores D, Castaneda V, Tada M, Härtel S and Concha M L 2017 *Nature communications* **8** 15431
[21] Landau L, Pitaevskii L, Kosevich A and Lifshitz E 2012 *Theory of Elasticity* v. 7 (Elsevier Science)
[22] Morita H, Grigolon S, Bock M, Krens S G, Salbreux G and Heisenberg C P 2017 *Developmental cell* **40** 354–366
[23] Walcott S and Sun S X 2010 *Proceedings of the National Academy of Sciences* **107** 7757–7762 ISSN 0027-8424
[24] Maloney J M, Walton E B, Bruce C M and Van Vliet K J 2008 *Physical Review E* **78** 041923
[25] Banerjee S and Marchetti M C 2012 *Physical review letters* **109** 108101
[26] Campinho P, Behrndt M, Ranft J, Risler T, Minc N and Heisenberg C P 2013 *Nature cell biology* **15** 1405
[27] Labernadie A, Bouissou A, Delobelle P, Balor S, Voituriez R, Proag A, Fourquaux I, Thibault C, Vieu C, Poincloux R *et al.* 2014 *Nature communications* **5** 5343
[28] Mertz A F, Banerjee S, Che Y, German G K, Xu Y, Hyland C, Marchetti M C, Horsley V, Dufresne E R *et al.* 2012 *Physical review letters* **108** 198101
[29] Haase K and Pelling A E 2015 *Journal of The Royal Society Interface* **12** 20140970
[30] De R, Zemel A and Safran S A 2007 *Nature Physics* **3** 655
[31] De R, Zemel A and Safran S A 2008 *Biophysical journal* **94** L29–L31